Desalination 520 (2021) 115360

Contents lists available at ScienceDirect

Desalination

journal homepage: www.elsevier.com/locate/desal

True driving force and characteristics of water transport in osmotic membranes

Lianfa Song [a,*], Mohammad Heiranian [b], Menachem Elimelech [b]

[a] Department of Civil, Environmental, and Construction Engineering, Texas Tech University, Lubbock, TX 79409-1023, United States
[b] Department of Chemical and Environmental Engineering, Yale University, New Haven, CT 06520-8286, United States

HIGHLIGHTS

- No chemical potential gradient of water in osmotic membranes for diffusive transport.
- Concentration difference manifests itself as negative hydraulic pressure in membrane.
- Water in the membrane in FO/PRO is thermodynamically unstable and tends to cavitate.
- Collapse of water continuity in membrane can reduce water significantly.

flux

ARTICLE INFO

Keywords:
Osmotic membranes
Water flux
Chemical potential
Negative pressure
Water continuity
Cavitation

ABSTRACT

Diffusion cannot be a major water transport mechanism in osmotic membranes because of the lack of true water concentration gradient within the membrane. Due to the semipermeable property of osmotic membranes, water concentration in the membrane is virtually constant because of the absence of salts. The recently confirmed porous structure of the skin layer of osmotic membranes cannot support the basis to exclude bulk water flow in the membrane as assumed in the classic solution-diffusion model. Herein we demonstrate that the concentration difference of water at the membrane-solution interface manifests itself as a negative hydraulic pressure in the membrane. Hence, the only possible driving force for water movement in osmotic membranes is hydraulic pressure gradient. Osmotically driven membrane processes are characterized with negative pressure within the membrane below the water vapor pressure, inevitable leading to the formation of vapor or small bubbles within the membrane matrix. This phenomenon is expected to markedly reduce the effectiveness of osmotic pressure as a driving force for water transport. Delineation of the breakdown and possible restoration of water continuity under negative pressure is essential for proper understanding of the principles governing water transport in osmotic membranes.

1. Introduction

Osmotic membranes are membranes that reject ions, such as sodium and chlorine ions. Osmotic membranes differ from non-osmotic membranes in that osmotic pressure (an expression of chemical potential) is a major driving force for water transport, in addition to hydraulic pressure. Currently available osmotic membranes, which are widely used in the processes of reverse osmosis (RO), forward osmosis (FO), and pressure retarded osmosis (PRO), are mostly made of polyamide (PA) or cellulose acetate (CA) materials. These osmotic membranes are often called semipermeable or permselective membranes because of their high permeability for water and ultra-high rejection rate of salts.

The high water-salt selectivity or separation efficiency of osmotic membranes is mainly attributed to the skin (active) layer of the membranes. The skin layer is commonly considered as a dense homogenous layer without voids or pores [1–3]. However, there were always opposite opinions that tiny pores exist in the skin layer of the membranes [4,5]. With advances in characterization techniques for the membrane structure over the years, it has become indisputable that the skin layer of both CA and PA osmotic membranes is porous in nature. The porous structures of skin layers were clearly captured in high-resolution TEM and SEM images [6–8]. The size and distribution of pores on the skin layer were analyzed and quantified with techniques such as small-angle neutron scattering (SANS) [6,9] and positron annihilation spectroscopy

* Corresponding author.
E-mail address: lianfa.song@ttu.edu (L. Song).

https://doi.org/10.1016/j.desal.2021.115360
Received 28 July 2021; Received in revised form 14 September 2021; Accepted 14 September 2021

(PALS) [10,11]. The voids of the PA layer of thin-film composite membranes were found to constitute 10–30% of the layer volume [11–13].

Of great interest is the calculation of water flux across osmotic membranes under various operating conditions. The mechanisms for water transport are believed to strongly relate to the structure and properties of the membranes and highly depend on the nature of the driving forces. Many theories and models were proposed to describe water transport in osmotic membranes [3,5,14]. Currently, diffusion is widely perceived and accepted as the predominant mechanism for water transport in these membranes. However, the theory or model of diffusive transport of water in membranes was conceptualized and developed over half century ago, at the early stage of osmotic membrane technology. It is the time now to rigorously revisit the assumptions and derivations used in the development of the theory or model for water transport in osmotic membranes. Considering the tremendous progress in osmotic membrane technologies made over this period, a better description of the subtle features of water transport in osmotic membranes is of paramount importance.

The objective of this paper is to refine and advance our understanding of the principles for water transport in osmotic membranes with the newly acquired knowledge in this field. First, the possible driving forces for water transport in osmotic membranes are examined and scrutinized with fundamental principles. Second, a new feature of water transport in osmotically driven membrane processes and its possible impacts on water flux are elaborated and discussed.

2. Chemical potential of water in the membranes

Diffusion and convection are two possible forms of water transport in osmotic membranes. The classic solution-diffusion model treats diffusion as the sole mechanism of water transport in the membrane [3,15]. In this model, the membrane is deemed as a dense layer of homogeneous (continuous) medium. Water first dissolves as dispersed phase on one side of the membrane. Then, water molecules diffuse to the other side of the membrane and dissociate from the membrane. Though solution-diffusion model might be a suitable model for gas transport in thin films and has enjoyed tremendous success in gas separation, it is too primitive to describe water transport in osmotic membranes. As we show later, the assumptions and derivations for the model are questionable or even inappropriate when they are rigorously scrutinized.

2.1. Definitions of chemical potential

The driving force for water diffusion is the gradient of water concentration (or more accurately activity) in the membrane. The direction of water movement is from high concentration to low concentration (downgradient). The driving force for diffusion can also be expressed in term of the chemical potential of water, which is defined as

$$\mu = \left(\frac{\partial G}{\partial n}\right)_{T,P} \tag{1}$$

where μ is the chemical potential of water (J/mol), G is the Gibbs free energy (J), and n is the number of water molecules (mol). The chemical potential is the Gibbs free energy per mole of water. This strictly defined chemical potential is related to concentration by

$$\mu = \mu^0 + RTln\frac{C}{C^0} = \mu^0 + RTlnX \tag{2}$$

where μ^0 is the chemical potential of pure water, R is gas constant (8.314 J/mol·K), T is the absolute temperature (K), C and C^0 are the water concentrations in solution and pure water (mol/m^3), respectively, and X is the mole fraction of water. The strict chemical potential is a function of water concentration.

For convenience, the chemical potential of water is sometime given in the "extended" form that includes free energy contribution from external fields. For example, in the membrane device shown in Fig. 1, the extended chemical potential of water is written as

$$\mu = \mu^0 + RTlnX + \widehat{V}_w P + \widehat{V}_w \rho g h \tag{3}$$

where $\widehat{V}_w$ is the molar volume of water (m^3/mol), P is the applied pressure on water (Pa), ρ is the density of water (kg/m^3), g is the gravitational acceleration (9.8 m/s^2), and h is the height of water (m). The second and third terms on the righthand side of Eq. (3) account for the contributions to the free energy from the pressure field and gravity field, respectively. Hydraulic pressure and gravity force are external forces that cause bulk flow of the whole solution but do not contribute to diffusive movement of water. Usually, the gravity force is negligible compared to the pressure in most cases.

2.2. A misstep in the solution-diffusion model

In general, water flux in the direction perpendicular to a membrane can be written as

$$J = -D\frac{\partial C}{\partial x} + vC \tag{4}$$

where J is the water flux (mol/m^2-s), D is the diffusion coefficient of water (m^2/s), x is the coordinate perpendicular to the membrane surface (m), and v is the bulk velocity of water (m/s). The first term on the righthand side of Eq. (4) is the diffusive component due to concentration gradient while the second term is the convective component due to the external fields (mainly pressure gradient). The solution-diffusion model assumes no pressure gradient in the membrane and, therefore, no convective flow. The water flux equation then reduces to

$$J = -D\frac{dC}{dx} \tag{5}$$

Eq. (5) is the well-known Fick's law, which means water transport is achieved by diffusion (random movement of water molecules) driven solely by concentration gradient.

The original derivation of the solution-diffusion model [15] started with Fick's law, Eq. (5), with concentration gradient of water as the only driving force. The driving force was then replaced with the strict chemical potential defined by Eq. (2). However, later in the derivation,

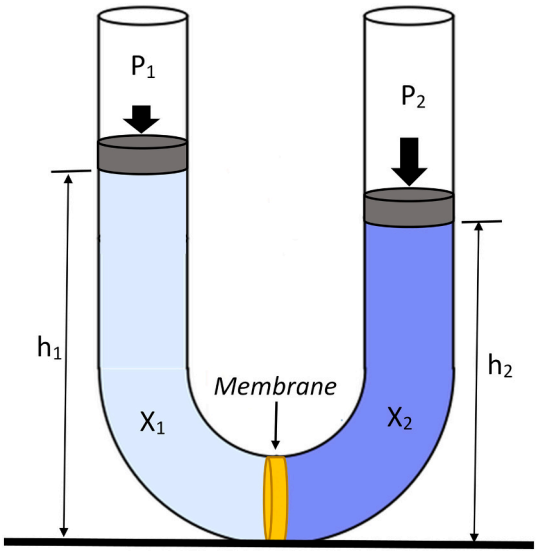

Fig. 1. Schematic of a membrane device with an osmotic membrane at the bottom to separate two solutions with different water concentration, hydraulic head, and pressure.

the extended chemical potential, as defined by Eq. (3) (without the gravity term), was erroneously substituted for the strict chemical potential in the derived equation. In this way, hydraulic pressure was introduced into the equation so that the well-established phenological equation for water flux in RO processes was reproduced:

$$J = A(\Delta P - \Delta\pi) \tag{6}$$

where A is the water permeability of membrane, and ΔP and $\Delta\pi$ are the hydraulic pressure difference and osmotic pressure difference across the membrane, respectively. Eq. (6) is a form of Darcy's law for water transport in porous media as applied to membrane filtration.

The above derivation is obviously inappropriate. Eq. (5) states clearly that water transport is driven only by concentration gradient. If Fick's law is accepted as the starting point, there should be no room to include hydraulic pressure as the driving force in any fashion. In other words, the popular Darcy's law, Eq. (6), for water flux in membranes cannot be derived rigorously from Fick's law, Eq. (5).

The change of chemical potential expressions introduces a dilemma in the solution-diffusion model about the hydraulic pressure. The basic assumption for the model is that water transport is solely driven by concentration gradient. However, hydraulic pressure difference ΔP appears in the final expression for water flux as a driving force of the same importance as the osmotic pressure difference $\Delta\pi$, which is an expression for the chemical potential of water. Such a contradiction between the final conclusion and the initial assumption appears to be a result of erroneous steps in the derivation.

A possible explanation for this misstep was the introduction of the concept of "pressure-induced diffusion" [3,16–18]. It was argued that the hydraulic pressure difference across the membrane would reduce water concentration on the low-pressure side of the membrane, such that the pressure difference between the membrane surfaces could be converted to concentration gradient of water within the membrane. This mechanism was invoked to justify the assumption that diffusion is the sole mechanism for water transport in the membrane. Pressure induced diffusion may not be a problem for gas transport in membranes because the concentration of a gas is directly related to pressure. However, there are no fundamental theories or principles to support the reduced water concentration at the lower pressure side of a membrane.

2.3. State of water and chemical potential

Instead of water concentration gradient, the gradient of water (or solvent) fraction in the membrane was often used as driving force for water (or solvent) diffusive transport, implying that chemical potential of water is proportional to water (or solvent) fraction in a membrane [2,15,19]. This can be misleading if the state of water in the membrane is not clearly specified. When water exists as a liquid phase (condensed state), water fraction is an extensive property that does not affect the chemical potential of water because the latter is a function of concentration, which is an intensive property. As shown schematically in Fig. 2, there are wedge-type pores with decreasing size from one side to the other side of a membrane. Although water fraction changes across the membrane thickness, there is no driving force for diffusive transport of water because the chemical potential of the water is equal throughout the membrane thickness.

Water fraction in the membrane can be an intensive property when there is salt dissolved in water or if water dissolves as dispersed state in the membrane. Because osmotic membranes are an excellent barrier to salt, it is reasonable to assume negligible amount of salt in water inside the membranes. In the solution-diffusion model, water is considered to dissolve in the membrane as dispersed state so that it moves in the membrane through diffusion rather than viscous bulk flow.

If water truly disperses as freely moving molecules when it enters the membrane, evaporation (latent) heat would be consumed. Therefore, the temperature would drop significantly when a piece of membrane is submerged in water in a thermally isolated container. The temperature change should be easily detected because of the large latent heat (2441.7 kJ/kg) and the relatively small (isobaric) specific heat capacity (4.18 kJ/kg·K) of water (e.g., at 25 °C), respectively. Of course, it is arguable if the dissolution of water in the membrane can be an isothermal or exothermic process, in which water molecules form strong bonds with sites of the membrane matrix that release equal or more heat than the evaporation heat. However, in that case, the molecules would not be freely movable as needed for water transport across the membrane.

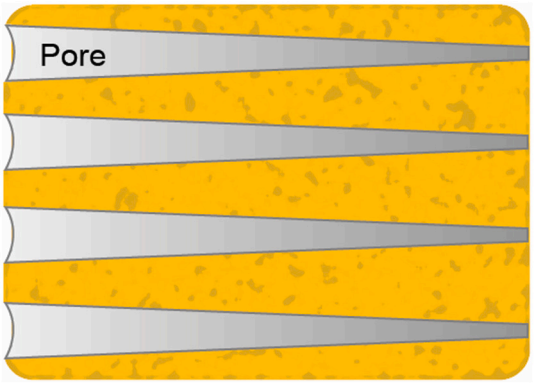

Fig. 2. Schematic of a membrane with wedge-type pores from one side to the other side. No chemical potential gradient of water exists across the membrane thickness.

Because there are strong attractive intermolecular forces between water molecules, vapor tends to condense to liquid water at a relatively very low concentration. Vapor pressure of water at 25 °C is 0.0317 bar. Assuming it follows ideal gas behavior, the volume fraction of water in vacuum or air is calculated by

$$w = \frac{P_v}{RT} \times \hat{V}_w = \frac{0.0317\text{bar}}{8.314 \times 10^{-5}\text{m}^3\text{bar}/\text{mol}\cdot\text{K} \times 298\text{K}} \times 1.8 \times 10^{-5}\text{m}^3 \Big/ \text{mol} = 2.30 \times 10^{-5} \tag{7}$$

where w is the water (volume) fraction and P_v is the vapor pressure of water. The result shows that the volume fraction of water in vacuum or air at most is only about 23 ppm in the dispersed state (vapor). Any excessive water molecules in air and vacuum must condense to liquid state due to the intermolecular forces between them. Considering a water fraction of 10% to 30% in osmotic membranes (based on typical membrane void fraction), there must be extremely strong forces in the membrane matrix opposing the intermolecular attractive forces between water molecules if such a large amount of water was maintained in dispersed state. Unless there is a strong support for the existence of such forces, it would be more reasonable not to treat water as dispersed state in osmotic membranes.

3. The sole driving force for water transport

It is argued in the previous section that water in the membrane mainly exists in continuous condensed (liquid) state. Furthermore, salt concentration in osmotic membranes is negligible because the membrane is an excellent barrier to salt. Therefore, there is no chemical potential gradient of water in the membrane. It can be seen from Eq. (4) that water transport in the membrane can only be in the form of bulk flow, driven by the gradient of hydraulic pressure. The recently confirmed porous structure of the skin layer of osmotic membranes [6–8] has removed the barrier for considering bulk flow of water in osmotic membranes.

The claim of hydraulic pressure gradient as the sole driving force for water transport in osmotic membranes is readily acceptable for RO because the net driving force is hydraulic pressure. But what is the mechanism of water transport in FO and PRO where the net driving force is osmotic pressure? This question is answered below.

3.1. Thermodynamic equilibrium at the interface

Concentration difference of water at the surface of a membrane cannot directly build up a concentration gradient within or across the membrane, but it can induce a hydraulic pressure gradient in the membrane. Taking an FO process as an example, in which a membrane separates pure water and a salt solution, with no hydraulic pressure applied on either side of the membrane, the extended chemical potentials of water in the membrane and in the solution at the interface can be written as [20,21].

$$\mu_m = \mu^0 + \widehat{V}_w P \ (in\ membrane) \tag{8}$$

$$\mu_s = \mu^0 + RTlnX = \mu^0 - \widehat{V}_w \pi \ (in\ solution) \tag{9}$$

where μ_m and μ_s are the extended chemical potentials of water in the membrane and in the solution, respectively, and P and π are the hydraulic pressure in the membrane and the osmotic pressure in the solution at the interface, respectively. Because the membrane is impermeable to salts, the molar concentration of water in the membrane is unity, and the concentration related term in Eq. (8) vanishes. Moreover, the pressure term drops out of Eq. (9) because no hydraulic pressure is applied on the solution. Eq. (9) also shows that the existence of salt in the solution ($X < 1$) reduces the chemical potential of water by a value of $\widehat{V}_w \pi$. The gravity term does not appear in either equation because the same heights of water level are assumed so that they cancel each other.

At equilibrium, the extended potentials of water in membrane and in solution are equal at the interface. Hence, a negative hydraulic pressure must be induced in membrane at the interface that is equal in magnitude to the osmotic pressure of the solution:

$$P = -\pi \tag{10}$$

Because there is no pressure initially applied on the pure water in the FO process, a gradient of hydraulic pressure in the membrane toward the solution develops by the induced negative pressure at the interface with the solution. Water moves from the pure water to the solution under this pressure gradient. Similarly, it can be shown that a pressure gradient is developed in the membrane by a negative pressure at the interface in a PRO process.

3.2. Demonstration of the negative hydraulic pressure

The induced negative pressure in the membrane at the interface with solution is not only a theoretical deduction from thermodynamics principles, but also can be determined with a simple filtration experiment, as demonstrated in the classic work of Mauro [22]. The device, shown in Fig. 3, is made of a cylinder with a membrane fixed somewhere in the middle. The cylinder is filled with pure water on the left side and salt solution on the right side, sealed with freely moveable pistons on both ends. A spring is attached to the piston on the pure water end. No other forces are added on the pistons. After the start of filtration, water moves from the pure water side to the solution side of the membrane. The piston on the pure water end moves rightward and the spring is expanded. The spring exerts a force on the piston to resist its movement. It is obvious that the pure water in this case is under tension and the pressure on it is therefore negative. Equilibrium is achieved when water movement stops, indicating that the force exerted by the piston on the pure water is equal to the drawing force from solution on the other side of the membrane, which is equivalent to the osmotic pressure of the solution. This idea, based on the classic experiment of Mauro [22], presents an alternative method for the measurement of osmotic pressure. Notably, the more common method for osmotic pressure measurement is to measure the positive pressure added on the solution side of the membrane at equilibrium.

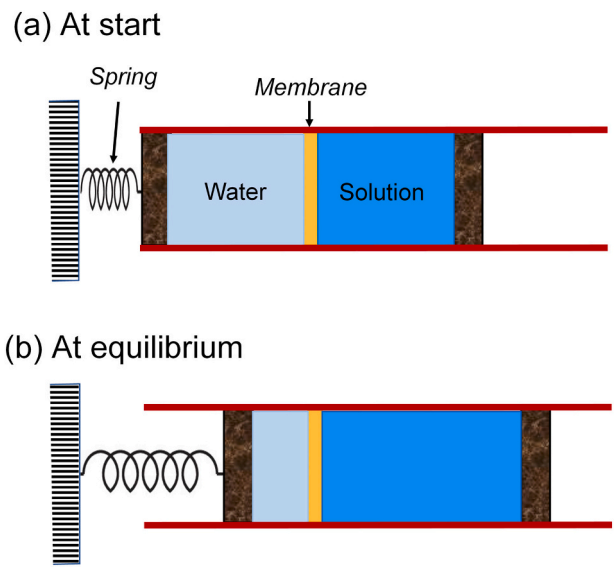

Fig. 3. Schematic of a membrane device to demonstrate the negative hydraulic pressure induced by water concentration difference at the interface of a membrane with solution. (a) At the start and (b) at equilibrium.

If salt concentration in the solution is maintained constant (e.g., by adding salt accordingly or circulating solution from a large reservoir), the hydraulic pressure profile across the membrane thickness at different times is schematically presented in Fig. 4. The profiles show a pressure gradient in the membrane toward the solution, which drives water from pure water to solution. The pressure gradient decreases with time as the negative pressure is built up on the pure water side. At equilibrium (no water flow), the pressure on the pure water is equal to the pressure in the membrane at the interface with solution, and the pressure gradient in the membrane vanishes. The invariant salt concentration in solution is used in the discussion only for convenience to

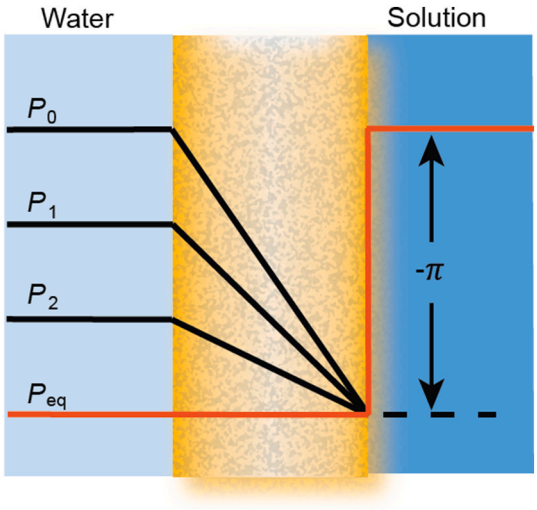

Fig. 4. Pressure profiles across a membrane in contact with a salt solution at different times of filtration. P_{eq} indicates equilibrium state when the pressure on the pure water is equal to the pressure in membrane at the interface with solution, which is equivalent to the osmotic pressure of the solution.

construct the pressure profiles in Fig. 4. It is always true that the negative pressure on the pure water at equilibrium is equal to the pressure in the membrane at the interface with solution.

3.3. Operation modes of osmotic membranes

An osmotic membrane can be operated in two different modes according to positive or negative hydraulic pressure in the membrane. The RO mode is characterized with a positive hydraulic pressure in the membrane, when the hydraulic pressure difference is greater than the osmotic pressure difference ($\Delta P > \Delta\pi$). The PRO mode is characterized with a negative hydraulic pressure in the membrane, when the osmotic pressure difference is greater than the hydraulic pressure difference ($\Delta\pi > \Delta P$). Pure water filtration ($\Delta\pi = 0$) and forward osmosis ($\Delta P = 0$) are the extreme cases of RO and PRO modes, respectively.

The linearity between water flux and net driving force as given by Eq. (6) has been satisfactorily verified in RO mode with experiments except for very high salt concentration (when the impact of concentration polarization may become significant) [23]. However, a strong nonlinearity between water flux and the net driving force appears when the membrane is operated in FO/PRO mode [24]. Water flux in PRO mode is usually much lower than that in RO mode under the same magnitude of net driving force.

This discrepancy between water fluxes in RO and PRO modes cannot be explained by different membrane permeabilities when the same membrane is being used. Internal concentration polarization (ICP) in the porous support layer of the membranes is commonly used to explain the low water flux and nonlinearity in PRO mode. However, the apparent paramount role of ICP on water flux might be substantially overestimated [25,26]. ICP can be minimized when the skin layer faces draw solution [24]. Furthermore, ICP can be completely eliminated with some FO membranes that are made without porous support layer. Nevertheless, water flux in FO remains low.

4. Controlling mechanism for water transport in FO/PRO mode

Depending on salt concentration in solution, the negative hydraulic pressure in the membrane operated in FO/PRO mode can be up to several tens of bars. Water under such conditions is thermodynamically unstable and tends to evaporate. A new phenomenon, cavitation, that is never encountered in RO mode could occur in the membrane under negative pressure. Water transport in FO/PRO mode is expected to be significantly affected by this phenomenon.

4.1. Cavitation in the membranes

Knowledge of two important properties of water is essential to understand the thermodynamic stability of water and the cavitation phenomenon in water. The first property of water is its ability to hold a certain amount of dissolved air in it. The amount of dissolved air in water at equilibrium (air solubility) under 1 atm pressure [27,28] is presented as a function of temperature in Fig. 5. The figure shows that air solubility decreases as temperature increases and significant amount of dissolved air exists in water at ambient temperature. It can be seen from Fig. 5 that there is about 17 l of dissolved air per cubic meter water at 25 °C. According to Henry's law, air solubility in water is proportional to the pressure applied on it. When the pressure decreases, the excess dissolved air will be released to form small bubbles in water. Applications of this principle can be found in canned carbonated beverages in the food industry and dissolved air flotation (DAF) operation for particulate removal in water and wastewater treatment.

Another important property of water is vapor pressure. If water does not fully occupy a closed space, there is always vapor (gas phase of water) to fill the rest of the space. The vapor pressure of water is the pressure at which the gas phase is in equilibrium with the liquid phase. Water will evaporate into vapor when the pressure is below the vapor pressure while vapor will condense back to water when the pressure is above the vapor pressure. Vapor pressure of water as a function of temperature [29] is also presented in Fig. 5. Vapor pressure of water is relatively low at ambient temperature (only 0.0313 atm at 25 °C).

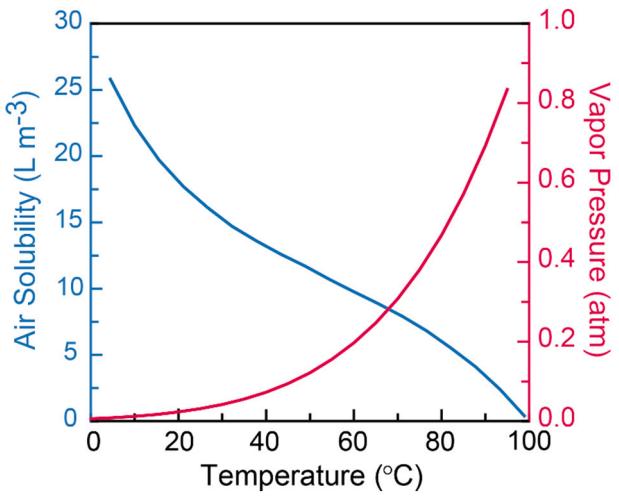

Fig. 5. Air solubility in water at 1 atm pressure and water vapor pressure at saturation as a function of temperature.

When pressure on water within the membrane drops to zero and below in FO/PRO mode, all the dissolved air must be released from water according to Henry's law. As a result, tiny bubbles form in water. The bubbles grow subsequently as water evaporates because the pressure on water within the membrane is lower than the water vapor pressure. This process is called cavitation. Cavitation is thermodynamically inevitable when the pressure is below the water vapor pressure. The initiation of cavitation is a dynamically difficult step that usually needs cavitation nuclei to start with. The tiny bubbles formed by the release of dissolved air provide the needed nuclei in this case.

4.2. Molecular dynamics simulations of bubble nucleation

A molecular dynamics (MD) simulation has been performed to investigate the possibility of bubble formation inside an osmotic membrane at the interface in contact with a high salt concentration solution. A 5 nm-long carbon nanotube (CNT) with a carbon center-to-center diameter of 1.08 nm (water accessible diameter of ~0.74 nm) was employed to simulate the pores in an osmotic membrane. The diameter of the pore is small enough so that no ions pass through the CNT. The simulation box consists of the CNT, two graphene sheets at the ends of the CNT, water molecules, and ions, as detailed in Fig. 6a. A nanopore with a diameter similar to that of the CNT is drilled in each graphene sheet. Details about the simulation methods and underlying principles are described in Appendix A.

The osmotic water transport is studied by calculating the variation of the number of water molecules in each reservoir. In our simulations, the salt (NaCl) concentrations at the high- and low-salt concentration reservoirs were 2 M and 0.1 M, respectively. As shown in Fig. 6b, water molecules are drawn to the high salt-concentration reservoir, as expected for an osmotic membrane.

During the simulation, no stable bubbles are observed for a long period of time. Therefore, we studied the probability of formation of nano-bubble nucleation (vapor phase) sites inside the CNT at its interface with the salt solution reservoirs. In Fig. 6c, the number of water molecules in small regions (σ) within 2 Å of each graphene wall is investigated. Here, vapor nucleation site is defined when the number of water molecules is less than the average number of water molecules within σ. The average number of water molecules within σ is 2.65. In Fig. 1c, the percentage of the simulation time for the observation of no

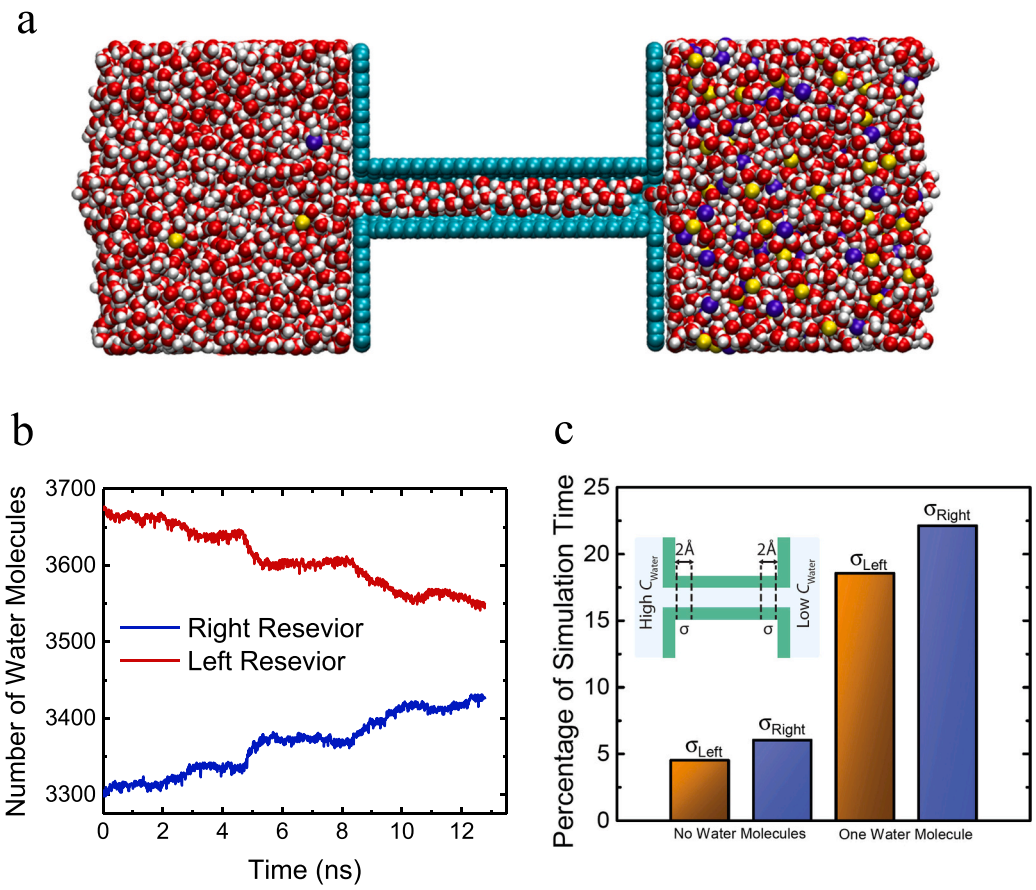

Fig. 6. (a) Snapshot of the simulation consisting of water (oxygen atoms in red and hydrogen atoms in white), sodium ions (in yellow), chloride ions (in blue), a CNT (carbon atoms in green), and graphene sheets (carbon atoms in green). Cut-through presentation of the CNT and graphene sheets is used to show the water molecules inside the membrane tube. (b) Variation of the number of water molecules in the two reservoirs with time, demonstrating the osmotically-driven flow of water molecules from the left reservoir to the right reservoir. (c) Percentage of the simulation time that the number of water molecules within 2 Å of the graphene sheets is less than 1 (i.e., zero) or equal to 1. The average number of water molecules within σ is 2.65. (For interpretation of the references to colour in this figure legend, the reader is referred to the web version of this article.)

water molecules as well as the observation of a single water molecule within each σ region is calculated. No water is observed for 4.53% and 6.04% of the time within σ near the low- and high-salt concentration interfaces, respectively. It is noted that over one-million-time frames are considered to obtain statistically reliable time percentages. The results show that although the membrane is structurally symmetric, the probability of formation of a vapor nucleation site near the high salt-concentration interface (where the negative pressure is induced) is higher than that of a nucleation site forming near the low salt-concentration interface. Hence, the MD simulation supports our mechanism of bubble formation outlined in the previous subsection.

4.3. Water flux in FO/PRO mode

Because membrane processes in FO/PRO mode are characterized concurrently with low water flux and inevitable cavitation, it is reasonable to wonder if there are fundamental connections between these two phenomena. In FO/PRO mode, water on the feed side is "drawn" by a solution from the draw side of the membrane. Water continuity in the membrane is critical for the drawing force to be effective. As schematically shown in Fig. 7, water continuity may break in some pores of the membrane due to the formation of air/vapor bubbles. As a result, less pores may be available for water transport in FO/PRO mode compared to RO mode. This mechanism contributes to the lower water flux in FO/PRO mode than that observed in RO mode. The collapse of water continuity in the membrane was not realized and postulated as a possible cause for low water flux in FO/PRO mode until very recently [21,30,31].

Water transport in FO/PRO mode is obviously controlled by more complex mechanisms than in RO mode. Cavitation starts when negative pressure on water builds up within the membrane. Then cavitation stops at a point and the process reverses when the negative pressure

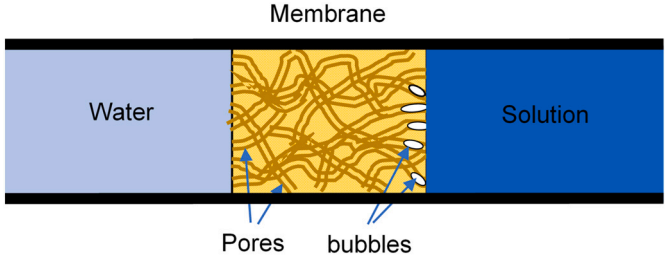

Fig. 7. Water transport under negative pressure may be hindered by the formation of air/vapor bubbles in the pores. Bubbles may form preferably in a region close to solution due to higher negative pressure.

disappears due to the collapse of water continuity, which is a consequence of cavitation. Bubbles may also move out of the membrane with water flow and accumulate at the interface of the support layer of asymmetric or thin-film composite membranes. The dynamics of alternating breakage and restoration of water continuity is postulated to play an important role in water transport in osmotically driven membrane processes.

As a newly realized phenomenon, to date, there is lack of knowledge about cavitation dynamics in membranes. At this moment, it is reasonable to suggest intuitively that a factor should be added in Eq. (6) to account for the impact of cavitation on water flux [21]:

$$J = A(1-\lambda)(\Delta\pi - \Delta P) \tag{11}$$

where λ is the fraction of the membrane (pore) area that is unavailable for water transport due to cavitation or bubble formation. The positions of hydraulic pressure ΔP and osmotic pressure $\Delta\pi$ is exchanged in Eq. (11) to produce a positive water flux in PRO mode (or FO mode when

$\Delta P = 0$). The extent of cavitation is expected to be affected by membrane properties, water chemistry, and operating conditions. Note that the pressure ΔP in Eq. (11) is the hydraulic pressure applied on the draw solution, which retards the water flux. The hydraulic pressure is much more effective to drive water through the membrane when it is applied on the feed water, like in RO, because water transport is not affected by cavitation [30].

Eq. (11) suggests a general approach to account for the effect of cavitation on water flux in PRO and FO modes. To accurately calculate the water flux, the effects of internal and external concentration polarization should also be included. The support layer of osmotic membranes induces internal concentration polarization which is much more severe than external concentration polarization because of the lack of mixing within the support layer. Based on our discussion above, bubbles forming the active later may be carried with the convective flow and accumulate in the support layer region near to the active layer, thus exacerbating internal concentration polarization due to the reduction of support layer effective porosity and water continuity. Studies on support layer chemical medications have shown that water flux in FO significantly increases when the support layer becomes more hydrophilic [32,33]. It is likely that the hydrophilic support layers can more effectively displace the accumulated bubbles (which are hydrophobic) by the convective flow than hydrophobic support layers.

5. Conclusion

Water transport in osmotic membranes cannot be achieved by diffusion because water in the membrane cannot constitute a true concentration gradient across the membrane. Instead, the concentration difference of water at the membrane interface manifests itself as a negative pressure in the membrane that is able to generate a gradient of hydraulic pressure in the membrane. Therefore, water movement in the membrane is driven solely by a hydraulic pressure gradient, regardless whether the original driving force is chemical potential (concentration) or hydraulic pressure.

Water flux under net hydraulic pressure (RO mode) is reasonably well described by Darcy's law. However, water transport under net osmotic pressure (FO/PRO mode) is controlled by more complex mechanisms. In FO/PRO mode, water in the membrane is thermodynamically unstable and tends to evaporate because of the negative pressure. With the ubiquitous dissolved air in water, cavitation is virtually inevitable in the membrane, resulting in breakage of the continuity of water across the membrane. The effectiveness of osmotic pressure for water transport can be substantially weakened by cavitation.

The collapse of water continuity due to cavitation in osmotically driven membrane processes is a newly recognized mechanism to affect water transport in membranes, which is most likely a major cause for the low water flux and nonlinearity in these processes, in addition to the extensively investigated phenomenon of internal concentration polarization. More research efforts are needed to delineate the features of the collapse and possible restoration of water continuity under negative pressure in osmotic membranes. A thorough understanding of this mechanism is of crucial importance to the construction of sound fundamental theories for water transport in osmotic membranes and for the development of osmotically-driven membrane processes with much higher efficiencies.

CRediT authorship contribution statement

Lianfa Song: Conceptualization, Methodology, Writing – Original Draft. **Mohammad Heiranian**: Formal analysis, Investigation. **Menachem Elimelech:** Writing- Reviewing and Editing.

Declaration of competing interest

The authors declare that they have no known competing financial interests or personal relationships that could have appeared to influence the work reported in this paper.

Appendix A. Simulations methods

MD simulations were performed using the LAMMPS package [34]. The simulation box in Fig. 1 contains 7052 water molecules, 458 ions, and 2576 carbon atoms. The system dimensions are 5 nm, 5 nm, and 15 nm in x, y, and z, respectively. The z axis is along the axis of the CNT. Periodic boundary conditions were applied in the x and y directions. The water reservoirs are ionized by Na^+ and Cl^- ions with a concentration of 0.1 M and 2 M. The SPC/E water model was used and the SHAKE algorithm was employed to maintain the rigidity of the water molecule. The interactions between carbon atoms and water molecules were modeled by the force-field parameters given in Wu et al. [35]. The effect of membrane flexibility was ignored for simplicity and the carbon atoms of the CNT and graphene sheets were fixed. For the ion-ion interactions and the interactions of ions with water and carbon atoms, the mixing rule was employed [36]. The Lennard-jones cutoff distance was set to 12 Å. The long range electrostatic interactions were computed by the Particle-Particle-Particle-Mesh (PPPM) method [37]. The energy of the system was minimized for 10,000 steps. Each solution next to a non-porous graphene sheet was equilibrated using NPT ensemble for 1 ns at a pressure of 1 atm and a temperature of 300 K with a time-step of 1 fs. Temperature was maintained at 300 K by using the Nosè-Hoover thermostat with a time constant of 0.1 ps [38,39]. Water was allowed to reach its equilibrium density (1 g/cm^3) in the NPT simulation. NVT simulation was then performed for 1 ns to further equilibrate the system. The final production simulation was performed in NVT ensemble for ~13.5 ns. To collect adequate statistics, the trajectories of the atoms were dumped every 20 femtoseconds.

References

[1] R. Riley, J.O. Gardner, U. Merten, Cellulose acetate membranes: electron microscopy of structure, Science 143 (1964) 801–803.
[2] H.K. Lonsdale, U. Merten, M. Tagami, Phenol transport in cellulose acetate membrane, J. Appl. Polym. Sci. 11 (1967) 1807–1820.
[3] J.G. Wijmans, R.W. Baker, The solution-diffusion model: a review, J. Membr. Sci. 107 (1995) 1–21.
[4] M. Mulder, in: Basic Principles of Membrane Technology, Kluwer Academic Publishers, 1996, pp. 52–59.
[5] A.F. Ismail, T. Matsuura, Progress in transport theory and characterization method of reverse osmosis (RO) membrane in past fifty years, Desalination 434 (2018) 2–11.
[6] S. Kulkarni, S. Krause, Investigation of the pore structure and morphology of cellulose acetate membranes using small-angle neutron scattering. 1. Cellulose acetate active layer membranes, Macromolecules 27 (1994) 6777–6784.
[7] L. Lin, R. Lopez, G.Z. Ramon, O. Coronell, Investigating the void structure of the polyamide active layers of thin-film composite membranes, J. Membr. Sci. 497 (2016) 365–376.
[8] Z. Zhang, Y. Qin, G. Kang, H. Yu, Y. Jin, Y. Cao, Tailoring the internal void structure of polyamide films to achieve highly permeable reverse osmosis membranes for water desalination, J. Membr. Sci. 595 (2020), 117518.
[9] X. Lu, M. Elimelech, Fabrication of desalination membranes by interfacial polymerization: history, current efforts, and future directions, Chem. Soc. Rev. 50 (2021) 6290.
[10] J. Li, B. Xiong, C. Yin, X. Zhang, Y. Zhou, Z. Wang, P. Fang, C. He, Free volume characteristics on water permeation and salt rejection of polyamide reverse osmosis membranes investigated by a pulsed slow positron beam, J. Mater. Sci. 53 (2018) 16132–16145.
[11] Z. Chen, K. Ito, H. Yanagishita, N. Oshima, R. Suzuki, Y. Kobayashi, Low energy positron annihilation study of composite reverse osmosis membranes, J. Phys. Conf. Ser. 262 (2011), 012013.
[12] M.M. Kłosowski, C.M. McGilvery, Y. Li, P. Abellan, Q. Ramasse, J.T. Cabral, A. G. Livingston, A.E. Porter, Micro- to nano-scale characterization of polyamide structures of the SW30HR RO membrane using advanced electron microscopy and stain tracers, J. Membr. Sci. 520 (2016) 465–476.
[13] X. Song, John W. Smith, J. Kim, N.J. Zaluzec, W. Chen, H. An, J.M. Dennison, D. G. Cahill, M.A. Kulzick, Q. Chen, Unraveling the morphology−function relationships of polyamide membranes using quantitative electron tomography, ACS Appl. Mater. Interfaces 11 (2019) 8517–8526.
[14] M. Soltanieh, W.N. Gill, Review of reverse osmosis membranes and transport models, Chem. Eng. Commun. 12 (1981) 279–363.
[15] H.K. Lonsdale, U. Merten, R.L. Riley, Transport properties of cellulose acetate osmotic membranes, J. Appl. Polym. Sci. 9 (1965) 1341–1362.

[16] S. Rosenbaum, O. Cotton, Steady-state distribution of water in cellulose acetate membrane, J. Polym. Sci. 7 (1969) 101–109.
[17] D.R. Paul, O.M. Ebra-Lima, Pressure-induced diffusion of organic liquids through highly swollen polymer membranes, J. Appl. Polym. Sci. 14 (1970) 2201–2224.
[18] M.A. Al-Obaidi, C. Kara-Zaitri, I.M. Mujtaba, Scope and limitations of the irreversible thermodynamics and the solution diffusion models for the separation of binary and multi-component systems in reverse osmosis process, Comput. Chem. Eng. 100 (2017) 48–79.
[19] D.R. Paul, Reformulation of the solution-diffusion theory of reverse osmosis, J. Membr. Sci. 241 (2004) 371–386.
[20] F. Kiil, Mechanism of osmosis, Kidney Int. 21 (1982) 303–308.
[21] H. Zhang, J. Wang, K. Rainwater, L. Song, Metastable state of water and performance of osmotically driven membrane processes, Membranes 9 (2019) 43.
[22] A. Mauro, Osmotic flow in a rigid porous membrane, Science 149 (1965) 867–869.
[23] S. Rosenbaum, W.E. Skiens, Concentration and pressure dependence of rate of membrane permeation, J. Appl. Polym. Sci. 12 (1968) 2169–2181.
[24] G.T. Gray, J.R. McCutcheon, M. Elimelech, Internal concentration polarization in forward osmosis: role of membrane orientation, Desalination 197 (2006) 1–8.
[25] S.S. Manickam, J. Gelb, J.R. McCutcheon, Pore structure characterization of asymmetric membranes: non-destructive characterization of porosity and tortuosity, J. Membr. Sci. 454 (2014) 549–554.
[26] A. Sagiv, P.D. Christofides, Y. Cohen, R. Semiat, On the analysis of FO mass transfer resistances via CFD analysis and film theory, J. Membr. Sci. 495 (2015) 198–205.
[27] R. Battino, T. Rettich, T. Tominaga, The solubility of nitrogen and air in liquids, J. Phys. Chem. Ref. Data 13 (1984) 563–600.
[28] Engineering ToolBox, Air solubility in water. https://www.engineeringtoolbox.com/air-solubility-water-d_639.html.
[29] D.R. Lide, in: CRC Handbook of Chemistry and Physics, 85th ed., CRC Press, 2004, pp. 6–8.
[30] N. Gao, J. Wang, L. Song, Independence of hydraulic pressures on the feed and draw solutions in the osmotically driven membrane processes, J. Membr. Sci. 586 (2019) 1–6.
[31] L. Song, Modeling and optimization of membrane process for salinity gradient energy production, Separations 8 (2021) 64.
[32] J.R. McCutcheon, M. Elimelech, Influence of membrane support layer hydrophobicity on water flux in osmotically driven membrane processes, J. Membr. Sci. 318 (2008) 458–466.
[33] J.T. Arena, B. McCloskey, B.D. Freeman, J.R. McCutcheon, Surface modification of thin film composite membrane support layers with polydopamine: enabling use of reverse osmosis membranes in pressure retarded osmosis, J. Membr. Sci. 375 (2011) 55–62.
[34] S. Plimpton, Fast parallel algorithms for short-range molecular-dynamics, J. Comput. Phys. 117 (1995) 1–19.
[35] Y.B. Wu, N.R. Aluru, Graphitic carbon-water nonbonded interaction parameters, J. Phys. Chem. B 117 (2013) 8802–8813.
[36] I.S. Joung, T.E. Cheatham, Determination of alkali and halide monovalent ion parameters for use in explicitly solvated biomolecular simulations, J. Phys. Chem. B 112 (2008) 9020–9041.
[37] T. Darden, D. York, L. Pedersen, Particle mesh ewald method for ewald sums in large systems, J. Chem. Phys. 98 (1993) 10089–10092.
[38] S. Nose, A unified formulation of the constant temperature molecular-dynamics methods, J. Chem. Phys. 81 (1984) 511–519.
[39] W.G. Hoover, Canonical dynamics - equilibrium phase-space distributions, Phys. Rev. A 31 (1985) 1695–1697.